VU Research Portal

Error and post-error processing in children with attention-deficit/hyperactivity disorder

Janssen, T. W.P.; van Atteveldt, N.; Oosterlaan, J.

Link to publication in VU Research Portal

citation for published version (APA)
Janssen, T. W. P., van Atteveldt, N., & Oosterlaan, J. (2020). Error and post-error processing in children with attention-deficit/hyperactivity disorder: An electrical neuroimaging study. *Clinical Neurophysiology*, *131*(9), 2236-2249. https://doi.org/10.1016/j.clinph.2020.06.022

Error and post-error processing in children with attention-deficit/hyperactivity disorder: An electrical neuroimaging study

T.W.P. Janssen [a,*], N. van Atteveldt [a], J. Oosterlaan [a,b]

[a] Vrije Universiteit, Clinical Neuropsychology Section, Van der Boechortstraat 7, 1081 BT Amsterdam, the Netherlands
[b] Emma Children's Hospital, Amsterdam UMC, University of Amsterdam, Emma Neuroscience Group, Department of Pediatrics, Amsterdam Reproduction & Development, Amsterdam, the Netherlands

HIGHLIGHTS

- Error (Ne, Pe) and post-error processing (N2) in ADHD were explored with source-reconstructed ERPs.
- Evidence was found for deficient adaptive control (reduced Pe) in the dorsal posterior cingulate cortex.
- Only controls showed a neural signature (N2 increase) of post-error processing in the left ventrolateral prefrontal cortex.

ABSTRACT

Objective: Inaccurate and inconsistent response styles in attention-deficit/hyperactivity disorder (ADHD) have been observed in a wide variety of cognitive tasks, in line with regulatory deficit models of ADHD. Event-related potential (ERP) studies of error processing have provided evidence for these models, but are limited in specificity. We aimed to improve the isolation, localization and identification of error (self-monitoring and adaptive control) and post-error (implementation of cognitive control) processing in ADHD.
Methods: ERPs were obtained for 46 ADHD and 51 typically developing (TD) children using the stop-signal task. Response-locked error (Ne and Pe) and stimulus-locked post-error (N2) components were compared between groups. Ne/Pe were corrected for preceding stimulus overlap and group differences were localized.
Results: Ne was intact, while Pe amplitude was markedly reduced in children with ADHD (ηp^2 = 0.14). Pe differences were localized in the dorsal posterior/midcingulate (BA31/24) cortex. While the TD group showed increased N2 amplitude in post-error trials (ηp^2 = 0.24), localized in the left ventrolateral prefrontal cortex (VLPFC) and angular gyrus, the ADHD group did not.
Conclusions: Self-regulation deficits in ADHD are associated with later stages of error processing and subsequent implementation of cognitive control.
Significance: We contribute to the literature by further specifying error processing deficits in ADHD.

© 2020 International Federation of Clinical Neurophysiology. Published by Elsevier B.V. All rights reserved.

1. Introduction

Children with attention-deficit/hyperactivity disorder (ADHD) are known for making "careless mistakes" and being "consistently inconsistent" (Kofler et al., 2013). This tendency for inaccurate (Rommelse et al., 2007) and inconsistent (Kofler et al., 2013) response styles has been observed in a wide variety of cognitive

tasks, rather than being confined to a specific task or cognitive function (e.g. inhibition). These cross-paradigm and cross-cognitive function findings have spurred the search for overarching explanations, such as in regulatory deficit models of ADHD (for a discussion, see Shiels and Hawk, 2010). According to these models, effective goal-directed behavior is dependent on *self-monitoring* and *adaptive control* processes. The former is needed to evaluate whether one's behavior is appropriate for the context, while the latter is crucial for adjusting one's behavior once a discrepancy is detected between the expected and actual outcomes. Deficits in

either of these processes may lead to maladaptive or suboptimal self-regulation, such as in ADHD.

Post-error slowing (PES) and post-error accuracy (PEA) are commonly used behavioral metrics for measuring self-regulation. PES describes the phenomenon of healthy people slowing down in the subsequent trial after committing an error (Rabbitt, 1966). By allowing more time for error processing, a more careful response style can be elicited to make the necessary adjustments after an error (to increase PEA). A recent meta-analysis demonstrated reduced PES in children and adults with ADHD (Balogh and Czobor, 2016). This finding may be explained by the more impulsive response style of people with ADHD, resulting in more premature responses, but without investing time in preventing future errors. PEA was not investigated in the meta-analysis, but many studies fail to find a correlation between PES and PEA (Ullsperger et al., 2014). Although PES is a useful metric to measure self-regulation, it is unsuitable to distinguish between more specific cognitive subcomponents such as self-monitoring and adaptive control. Electrophysiological measures of error processing have proven useful to study these processes more fine-grained.

With the event-related potential (ERP) technique, two components have been identified to map self-monitoring and adaptive control: error negativity (Ne) and error positivity (Pe), respectively. Ne (Falkenstein et al., 1991), also known as error-related negativity (ERN; Gehring et al., 1993), is a response-locked ERP that reaches a negative maximum around 50–100 ms after the initiation of an erroneous response. The Ne has a fronto-central scalp distribution and is presumably generated in the anterior cingulate cortex (ACC; Bush et al., 2000). At least four branches of theories attempt to explain what drives Ne (Wessel, 2012), including error detection/mismatch theories (Falkenstein et al., 1991; Coles et al., 2001) and conflict monitoring accounts (Botvinick et al., 2001; Yeung et al., 2004). The mismatch theory postulates that Ne reflects the amount of difference between an intended and the actually performed action, while the conflict monitoring theory postulates that Ne is not related to the accuracy of the response, rather it reflects the degree of motor response-conflict. The Ne is followed by a positive deflection, Pe, approximately 200–500 ms after the error, which has a centro-parietal topography. Where Ne is thought to be a more automatic process, Pe reflects conscious or emotional evaluation of the error (Nieuwenhuis et al., 2001). Unlike the Ne, the neural generators of the Pe are less well known, and are presumably more distributed (Wessel, 2012), including the ACC (Herrmann et al., 2004), posterior cingulate cortex (O'Connell et al., 2007; Vocat et al., 2008), and the parietal and insular cortices (Van Veen and Carter, 2002; Orr and Hester, 2012). The ambiguity related to the neural generators of Pe may also be the result of studies focusing on early or late parts of the Pe, which may have different functions and neural sources. Whereas the early Pe seems to be more related to the Ne and the ACC (Overbeek et al., 2005), the late Pe is potentially closer to the actual expression of error awareness (Endrass et al., 2007).

We identified 17 studies that reported group comparisons (ADHD versus typically developing children) of error-related ERP components, with all studies reporting on Ne and 14 studies on Pe, see Table 1. Nine of those studies reported reduced Ne amplitude in ADHD, while 7 did not demonstrate any Ne differences, and 1 study showed increased Ne amplitude. Of the 14 studies reporting Pe as well, 10 showed reduced Pe amplitude in ADHD, while 4 did not demonstrate group differences. Thus the existing literature shows considerable variation in findings pertaining to error-related ERP components in children with ADHD, although the evidence for a Pe reduction is probably more robust. This conclusion is largely in line with an earlier review on this topic based on nine studies in children (Shiels and Hawk, 2010). In addition, Ne and Pe abnormalities are reduced or even normalized by reward

(Groom et al., 2010; Rosch and Hawk, 2013) or treatment with stimulant medication (Groen et al., 2008; Groom et al., 2010) in children with ADHD, making these useful indices of treatment response. Interestingly, the effects of reward and stimulant medication on deficient error processing in ADHD, seem to have a basis in genetic polymorphisms associated with the brain's dopamine system, such as DAT1 10/10R (Althaus et al., 2010; Braet et al., 2011).

Functional magnetic resonance imaging (fMRI) studies of error processing in ADHD give additional insights in the underlying brain networks that may contribute to abnormal Ne and Pe components. Most consistently, studies report reduced activation in the ACC (Pliszka et al., 2006; Rubia et al., 2010; Braet et al., 2011; Rubia et al., 2011; van Rooij et al., 2015a), posterior cingulate cortex (Rubia et al., 2005, 2009, 2011), superior/medial frontal gyri (Rubia et al., 2010; Braet et al., 2011; van Rooij et al., 2015b), insula (Cubillo et al., 2010; Braet et al., 2011) and thalamus (Cubillo et al., 2010; Rubia et al., 2011). It should be noted, however, that most of these fMRI studies used a Go/Nogo or Stop Signal paradigm contrasting go and failed stop conditions, which does not isolate error processing from inhibition-related activation differences. Another caveat is that these fMRI studies cannot link the location of these brain activation differences to specific processes in time, such as Ne and Pe in ERP studies, due to low temporal resolution. ERP source localization methods can help to bridge the findings of high spatial resolution fMRI studies and the results of high temporal resolution ERP studies, increasing our detailed understanding of error processing deficits in ADHD.

Currently, no studies have used ERP source localization methods in children with ADHD to gain both temporal and spatial insights of deficient error processing. In contrast to the developmental literature, two studies explored the neural sources of Ne and Pe in adult ADHD using Go/Nogo tasks. One study found reduced early Pe amplitude in ADHD and concluded that this was attributable to reduced ACC activation (O'Connell et al., 2009). Another study identified the right insular cortex as source for Ne and Pe amplitude reductions in ADHD (Czobor et al., 2017). Both regions have been implicated as neural generators of Ne and Pe in healthy populations (Bush et al., 2000; Orr and Hester, 2012), while fMRI studies demonstrated reduced activation in ACC and insula in ADHD during error processing, as discussed. A few factors limit the interpretation of the source localization studies in adults with ADHD. First, stimulus-evoked activity may overlap with and confound the response-locked error components, resulting in residual inhibition-related processing. Second, one study did not perform a statistical group comparison on the source solution (Czobor et al., 2017), while the other implemented an equivalent current dipole method (O'Connell et al., 2009), which is more prone to operator bias and cannot handle multiple spatially extended sources.

In the current study we addressed several methodological limitations that we identified in the literature using the Stop-Signal Task (SST). First, we applied the "adjacent response filter method" (ADJAR; Woldorff, 1993) to remove stimulus-related overlap and improve isolation of response-locked error-related processes (see Bekker et al., 2005; Janssen et al., 2018 for a discussion and demonstrations). This is important in Go/Nogo and SST paradigms, especially given that ADHD is strongly associated with deficient response inhibition (Barkley, 1997). Second, we applied individual distributed source localization and statistically tested for group differences on the whole-brain level (similar to parametric maps in fMRI). Third, implementation of cognitive control in trials following errors has received little scrutiny. Behavioral post-error adjustments, such as PES (slowing) and PEA (accuracy) have not been reported in most ERP studies (only in 6 of 17 studies), and post-error ERP components have not yet been investigated in

Table 1
ERP studies of error processing in children with ADHD.

Study	N (group)	Age	Task	Manipulation	PES	Ne	Pe	Other results
Liao et al. (2018)	31 ADHD 12 TD	10	CPT	N/A	N/A	v	N/A	
Shephard et al. (2016)	11 ADHD 20 TD	13	Go/No-Go task	N/A	^	v	v	
Eichele et al. (2016)	39 ADHD 35 TD	10	Flanker task	N/A	=	=	=	
Rosch and Hawk (2013)	30 ADHD 25 TD	11	Flanker task	Motivation	N/A	v	v	Rewards enhanced error-related Pe amplitude in ADHD
Groom et al. (2013)	28 ADHD 28 TD	12	Go/No-Go task	Motivation Medication	N/A	v	v	Ne and Pe enhanced by MPH and incentives in ADHD
Senderecka et al. (2012)	20 ADHD 20 TD	9	Stop-signal task	N/A	N/A	v	v	
Sokhadze et al. (2012)	16 ADHD 16 TD	13	CPT	N/A	=	=	=	
Shen et al. (2011)	14 ADHD 14 TD	8	Stop-signal task	N/A	N/A	=	v	
Van de Voorde et al. (2010)	18 ADHD 16 TD	10	Go/No-Go task	N/A	=	=	v	
Zhang et al. (2009)	14 ADHD 14 TD	8	Go/No-Go task	N/A	N/A	=	v	
Albrecht et al. (2008)	68 ADHD 22 TD	11	Flanker task	N/A	N/A	v	=	
Groen et al. (2008)	35 s ADHD 18 TD	11	Probabilistic learning task	Medication	N/A	v	v	Medication normalized Ne and Pe.
Burgio-Murphy et al. (2007)	182 ADHD 29 TD	10	CPT	N/A	N/A	^	=	
Van Meel et al. (2007)	16 ADHD 16 TD	11	Flanker task	N/A	=	v	N/A	
Jonkman et al. (2007)	10 ADHD 10 TD	11	Flanker task	Medication	=	=	v	
Liotti et al. (2005)	10 ADHD 10 TD	11	Stop-signal task	N/A	N/A	v	N/A	
Wiersema et al. (2005)	22 ADHD 15 TD	10	Go/No-Go task and S1-S2 task	N/A	^	=	v	

Note. Other diagnostic groups, or comorbid groups, have been omitted for clarity. Significant reductions (v), increases (^), or similar (=) post-error slowing (PES), Ne or Pe. N/A = non-applicable; TD = typically developing; CPT = continuous performance task; ERP = event-related potential.

ADHD, even though these can improve our mechanistic understanding of how cognitive control is implemented at the neural level. We explored these components in line with Chang et al. (2014) who demonstrated that the stimulus-locked N2 component in go trials that follow error trials is sensitive to PES in healthy young adults. FMRI studies found PES to be associated with activity in the ventrolateral prefrontal cortex (VLPFC) (Li et al., 2008; Zhang et al., 2017).

Based on the literature we expected to find reduced Ne and Pe amplitudes in children with ADHD - being more confident to find Pe differences - accompanied by reduced post-error slowing and accuracy and N2 amplitude in go trials following stop errors. As for the underlying brain sources, we expected to find an ACC source for Ne differences, while such a specific hypothesis was difficult for Pe, considering the more extended brain network associated with this component. For N2, we expected to find sources in the VLPFC.

2. Methods

2.1. Participants

Complete data were available for 97 children (7–14 years) with 46 children in the ADHD group (37 males) and 51 children in the TD group (37 males; see Table 2). All participants were required to have an estimated full-scale IQ > 80 on the short version of the Wechsler Intelligence Scale for Children (WISC-III; Wechsler, 1991) based on subtests Arithmetic, Vocabulary, Block Design,

and Picture Arrangement. In addition, participants were excluded if there was a known history of neurological conditions.

In a previous study we described the enrollment of participants: "The ADHD group was recruited through mental health outpatient facilities in the West of the Netherlands. All children obtained a clinical diagnosis of ADHD combined type according to the Diagnostic and Statistical Manual of Mental Disorders (4th ed.; DSM-IV; American Psychiatric Association, 1994) as established by a child psychiatrist. This diagnosis was confirmed with the parent version of the Diagnostic Interview Schedule for Children (DISC-IV; Shaffer et al., 2000), and by parent and teacher ratings on the Disruptive Behavior Disorders Rating Scale (DBDRS; Pelham et al., 1992), which required at least one of the scores on the Inattention or Hyperactivity/Impulsivity scales to be in the clinical (>90th percentile) range for both informants. Seventy-six percent of children were naïve for stimulant medication and the remaining children discontinued the use of stimulants at least four weeks before testing. Children with a clinical DSM-IV diagnosis of autism spectrum disorder were excluded. The TD group was recruited through three primary schools and a sports club in the same recruitment area as the ADHD group. Control children were required to obtain normal scores on the DBDRS (<90th percentile) for both informants and to be free of any parent reported psychiatric disorder" (Janssen et al., 2016).

2.2. Procedure

This study was conducted in accordance with the Declaration of Helsinki, and approved by the local ethics committee before the start of the study. Parents and children (>12 years old) signed

Table 2
Group characteristics and task performance.

	ADHD		TD		Group difference	
	(*n* = 46)		(*n* = 51)			
	M	*SD*	*M*	*SD*	*F*(1,83) *p*	
Demographic data						
Age (years)	9.71	1.97	9.88	1.21	0.29	ns
IQ	99.76	12.37	110.56	14.40	15.54	<0.001
Gender (M/F)	37/9	N/A	37/14	N/A	0.83[a]	ns
DBDRS parents						
Inattention	17.35	5.20	3.69	3.40	239.11	<0.001
Hyperactivity/ Impulsivity	17.07	4.87	3.12	2.82	305.29	<0.001
DBDRS teacher						
Inattention	16.54	5.53	2.27	3.61	231.18	<0.001
Hyperactivity/ Impulsivity	16.48	6.66	1.59	2.64	217.53	<0.001
Stop-Signal Task						
pG (RT)	684.32	108.51	598.59	105.03	15.62	<0.001
pSE (RT)	658.52	112.27	588.03	96.84	11.02	0.001
pSEi (RT)	825.98	119.22	719.11	120.43	19.23	<0.001
pSEni (RT)	520.63	82.26	470.37	75.79	9.81	0.002
PES (pSE-pG)[b]	−25.81	72.96	−10.55	42.13	1.63	ns
pG accuracy (%)	92.65	4.77	95.32	3.06	10.96	0.001
pSE accuracy (%)	89.93	6.77	92.89	4.58	6.46	0.013
PEA (pSE-pG)	−2.72	4.49	−2.43	3.56	0.13	ns

Note. DBDRS = Disruptive Behavior Disorders Rating Scale; M = male, F = female; TD = typically developing; M = mean; SD = standard deviation; ns = not significant; pG = Go following Go; pSE = Go following stop errors [SE]; RT = reaction time; i = increase, ni = not increase; PES = post-error slowing; PEA = post-error accuracy (accuracy pSE-pG).
[a] $\chi^2(1)$.
[b] Please note that negative PES, means an actual acceleration of reaction times in go trials after stop errors, and negative PEA, means worse accuracy in go trials after stop errors.

informed-consent. The current study sample partly overlaps with a sample participating in a randomized controlled trial on the effects of neurofeedback, methylphenidate and physical exercise as interventions for ADHD (trial number: NCT01363544). Only pre-intervention data was used in the current study. The currently analyzed stop-signal task (SST) (30 minutes) was preceded by a resting state EEG recording (5 minutes eyes open, and 5 minutes eyes closed) and followed by an Oddball task (20 minutes), which are described elsewhere (Janssen et al., 2016, 2017).

2.3. Behavioral assessment

Parents and teachers completed the Strengths and Weaknesses of ADHD symptoms and Normal behavior scale (SWAN; Swanson et al., 2006; Arnett et al., 2013) containing two scales measuring attentional functioning (Attention scale) and impulse control (Impulse Control scale). The SWAN employs 18 items on a seven-point scale ranging from 'far below average' (3) to 'far above average' (−3), to allow for ratings of relative strengths as well as weaknesses on the two scales. Ratings on the SWAN were used for correlational analyses with the primary outcome measures.

2.4. Stimuli and task

The task has been described in a previous article: "The SST involved two types of stimuli: go stimuli and stop stimuli. Go stimuli were left or right pointing airplanes requiring either a left or right button response. Each trial started with a black fixation cross, centered on a white background for 500 ms, followed by a go stimulus for 1250 ms and a blank screen for 650 ms. Inter-trial-intervals varied randomly between 0, 50, 100, 150 and 200 ms. In a randomly selected 25% of the trials, go stimuli were followed by a visual stop signal (traffic stop sign) superimposed on the go stimulus, requiring the participants to withhold their response. The delay between the go and stop signal (Stop Signal Delay, SSD) varied trial-by-trial using a tracking algorithm which increased or decreased the delay with 50 ms, depending on

whether or not the previous stop trial resulted in successful inhibition. This procedure yielded approximately 50% successful stops and 50% stop errors.

Two practice runs (one containing 12 go trials and another containing 20 mixed go and stop trials) and 6 experimental runs of 100 trials were administered in 25 minutes with the trials presented in a fixed pseudorandomized order. Participants were instructed to respond both quickly and accurately to the go stimuli and withhold their response when a stop signal was presented. They were told that they would be unable to withhold their responses on all stop trials, and that they should not wait for the stop sign. The task was interrupted by two short breaks of one minute. Performance was monitored online in order to check the participant's co-operation and protocol adherence, and if needed, additional standardized instructions were given during the one-minute breaks" (Janssen et al., 2018).

Analysis of task performance was based on Chang et al. (2014), see Fig. 1 for an overview. First we distinguished the following trial types: correct go (G), incorrect go (F), stop success (SS) and stop error (SE). G trials were further divided based on the prior trial: pG, pF, pSS and pSE. For example, pSE (post stop error) trials were correct go trials that were preceded by SE trials. Within pSE trials, a distinction was made between trials that increased (pSEi) and not increased (pSEni) in reaction time (RT). To determine whether a specific pSE trial increased or did not increase, we compared it's RT with the average RT of all pG that preceded this particular trial within the run. With the i versus ni distinction, it is possible to investigate how PES is related to ERPs *within* participants. Dependent variables were: reaction time (ms) for the different trial types, post-error slowing (PES; RT pSE-pG), accuracy (%) for pG and pSE, and post-error accuracy (PEA; accuracy pSE-pG).

2.5. Electrophysiological recordings

EEG recording is similar to a previous study, which was described as follows: "Continuous EEG was recorded at 512 Hz using the ActiveTwo Biosemi system and ActiView software (Bio-
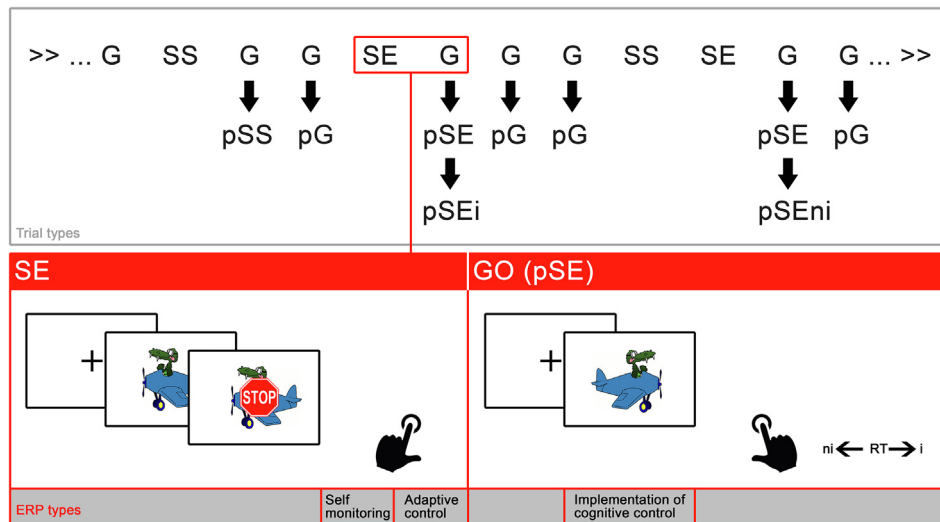
Fig. 1. Overview of trial types and event-related potential (ERP) types: (1) self-monitoring, (2) adaptive control and (3) implementation of cognitive control. *Note.* Trial types: G = go, SS = stop success, SE = stop error, trial types were subsequently divided based on what kind of trial preceded them, indicated with 'p' for post. pSE trials were also divided in whether reaction time (RT) increased (i) or not increased (ni). ERP analyses focused on SE and G (pSE) trial types. ERPs: Self-monitoring and Adaptive Control were response-locked, and Implementation of cognitive control was stimulus-locked. Trial types example was based on Chang et al. (2014).

semi, Amsterdam, The Netherlands) from 128 scalp electrodes according to the ABC labelling system, referenced to the active common mode and grounded to the passive driven right leg, which functions as a feedback loop to drive average potentials across electrodes to the amplifier zero. Electro-oculogram (EOG) was obtained using two electrodes at the external canthi, and two electrodes at infra- and supra-orbital sites.

Off-line analyses were performed with Brain Vision Analyzer 2 software (Brain Products, Gilching, Germany, Version 2.1). A Butterworth Zero Phase band-pass filter of 0.1–30 Hz at 24 dB/oct was applied, and scalp electrodes were re-referenced to the average of the mastoids. Broken electrodes were interpolated with the spherical splines method (Perrin et al., 1989). Ocular artifacts were estimated and corrected with a semi-automatic independent component analysis (ICA) using a restricted infomax algorithm (Jung et al., 2000), and automatic artifact rejection was applied to segments based on the following criteria: maximum allowed voltage step of 50 μV/ms, maximal peak-to-peak amplitude difference of ± 150 μV, and minimal low activity of 0.50 μV for 100 ms intervals" (Janssen et al., 2018).

The current study builds further on preprocessing steps that were applied in a former publication, which focused on the analysis of inhibition-related processes, as reflected in stop stimulus-locked N2 and P3 components (Janssen et al., 2018). Current analyses were performed separately for response-locked (G and SE) and stimulus-locked ERPs (correct go trials with preceding go or stop error trials: pG and pSE). The focus of response-locked ERPs was on error-related control processes (self-monitoring and adaptive control) reflected in Ne and Pe, while the stimulus-locked analyses focused on post-error processes related to the implementation/outcome of the former control processes, as reflected in N2 (note, during go trials, not stop trials).

First, both G and SE trials were segmented from −200 to 600 ms relative to the button press (response-locked), and baseline-corrected for the interval −100 to 0 ms. Due to the adjacency between the stop stimulus and response during SE trials, inhibition-related processing induced by the stop stimulus overlaps with error-related processing induced by the response. This may confound the response-locked analysis, because both inhibition and error monitoring rely on prefrontal control processes (including the ACC, which is hypothesized to be involved in this study), and the former was demonstrated to differentiate ADHD

from typically developing children (Janssen et al., 2018). In addition, reaction times during SE trials are assumed to be faster than during G trials (Verbruggen et al., 2013), as demonstrated in this study (524 versus 605 ms), making the potential overlap even more problematic. We corrected for this overlap with ADJAR (Woldorff, 1993), which filters out overlap of previous events.

With ADJAR, for each participant a previous event distribution (stop-stimulus) was determined relative to the timing of the current event (response error). In other words, the current event is fixed in time, while the previous event varies in timing. Subsequently, a convoluted waveform was calculated by averaging the participants' successful stop ERP over the range of the event distribution. This convoluted waveforms was then extracted from the current event waveform (response-locked ERP), removing the overlap of the previous event. The result is mostly a low-pass filtering, as high-frequency components cancel each other out. For a theoretical discussion about convolution, see Luck (2014).

After this correction, a 100 ms pre-stimulus baseline was applied and averages were obtained for G and SE response-locked ERPs. We also calculated these ERPs separately for SE responses based on whether the RT on the following go trial increased or did not increase (pSEi vs pSEni trials, see section 2.4). Second, pG and pSE trials were segmented from −200 to 800 ms relative to the onset of the go stimulus (stimulus-locked), baseline-corrected for the interval −100 to 0 ms, and averages were obtained for pG and pSE. Again, ERPs were also calculated based on whether RT increased or not increased on the particular pSE trial.

Grand average ERPs, scalp topographies and difference waves for each trial type were inspected to define analysis windows for Ne (77–127 ms), Pe (420–520 ms) and N2 (373–398 ms). More specifically, for Ne, the 50 ms window was based on the latency of the electrode with highest amplitude in the TD group (C23; ± 25 ms), which was more pronounced than in the ADHD group, although no latency shift was apparent in the ADHD grand average. Pe was determined similarly, except that the average latency was used for the maxima of TD and ADHD (A5) as both groups had pronounced Pe peaks, and a larger window (±100 ms) was used. Ne and Pe windows were based on differences waves (SE-G). Finally, N2 was based on the maximal difference between pG and pSE for the TD group (B2), which was not visible in the ADHD group. We chose a smaller window (25 ms) due to the shorter duration of

the component. Mean voltage amplitudes were extracted and used for statistical analyses (Ne, Pe: G, SE, G-SE; N2: pG, pSE). A minimum of 20 artefact-free segments were required for each condition to be included.

2.6. LAURA source estimation

We have described LAURA in several previous papers: "LAURA is a source reconstruction method that incorporates biophysical laws to obtain the optimal solution that fulfills both the observed data and bio-electromagnetic constraints. In this approach, the relationship between brain activity at one point and its neighbors is expressed in terms of a local autoregressive estimator with coefficients depending upon a power of the distance from the point (Grave de Peralta Menendez et al., 2004). Cartool software uses the L-curve method to find the optimal regularization parameter for a given data file (Hansen, 1992). We used the Locally Spherical Model with Anatomical Constraints (LSMAC) as lead field model, which has been shown to perform as well as more computationally intensive models like the Boundary Element Model (BEM) (Birot et al., 2014). Inverse solutions were calculated for each participant and epoch separately on a realistic head model that included 5004 equally distributed nodes within the gray matter of the Montreal Neurological Institute (MNI) transformed NIHPD pediatric brain atlas based on 7.5–13.5 years old children (Fonov et al., 2009, 2011)" (Janssen et al., 2018).

2.7. Statistical analysis

Analyses were performed with SPSS 23 (IBM, 2015). Significance was assumed if $p < .05$ (two-tailed). Demographic data were compared between groups with one-way ANOVA or $\chi 2$ test with Fisher exact correction. For the main outcomes, mean difference and 95% confidence interval [95% CI] are reported. Effect sizes (Cohen, 1988) are reported as partial eta-squared (η_p^2), with effects interpreted as small (0.01), medium (0.06) or large (0.14).

For all ERP analyses, multivariate test statistics are reported, a method known to be robust against violations of sphericity (Vasey and Thayer, 1987). First, three GLM MANOVAs were performed to validate the different components (Ne, Pe and N2), using three within-subject factors: Condition (Ne and Pe analyses: G, SE; N2 analysis pG, pSE), Lateral (left, midline, right) and Sagittal (frontal, central, posterior). For these analyses 9 electrodes were used in a 3x3 grid (F3, Fz, F4, C3, Cz, C4, P3, Pz and P4). Some interactions that involved location were tested further, by averaging electrodes (e.g. average midline [Fz, Cz, Pz] versus average left [F3, C3, P3] versus average right [F4, C4, P4]).

Second, group differences were assessed with three GLM MANOVAs, using group as between-subject factor (TD, ADHD), and Location (Fz, Cz, Pz) as within-subject factor. We chose for midline electrodes to reduce complexity, which we deemed reasonable, based on: (1) the ERP literature, as we hypothesized maxima at midline electrodes: Fz for Ne (Gehring et al., 2018; Overbye et al., 2019), Cz/Pz for Pe (Ridderinkhof et al., 2009; Overbye et al., 2019) and Fz for N2 (Chang et al., 2014), (2) the ADHD/ERP literature (see Table 1), as most studies demonstrated maximal differences between groups at midline locations, (3) the validation of ERP component characteristics in the current study and, (4) the difference topographic maps (TD-ADHD) to check whether our data is in line with the ADHD literature and to ascertain we are not missing unexpected differences in lateral locations. Furthermore, for Ne and Pe, we used the difference wave (SE-G), while for N2, we used another within-subject factor Condition (pG, pSE) to test for interactions between Group and Condition.

Partial Pearson correlations were calculated, separately for TD and ADHD, between performance, ADHD symptoms and ERP vari-

ables, controlling for age. To reduce the number of correlations, only electrodes with the maximum ERP amplitude were used (Fz for Pe and N2, Pz for Pe). P-values < 0.01 were considered significant.

For the LAURA source estimations, unpaired t-tests for each node were used to test for group differences. Based on Grave de Peralta Menendez et al. (2004), p-values were Bonferroni-corrected based on the number of electrodes ($p = .05/128 = 0.0004$). Coordinates were converted from MNI to Talairach space with the icbm2tal algorithm (Lancaster et al., 2007) using GingerALE software (Laird et al., 2005). Individual ROIs were computed for brain regions that differed significantly between groups by averaging nodes to obtain correlations with performance measures. Condition effects (pG, pSE) for N2 were tested with paired t-tests.

3. Results

3.1. Group characteristics and data quality

Table 2 summarizes the group characteristics. Groups did not differ in age or gender. As expected, IQ was lower in the ADHD group. Children with ADHD were slower and less accurate on all trial types, however PES and PEA were not different between groups. The GLM MANOVA demonstrated an overall medium-sized effect of Condition (pG, pSE) on RT, $F(1,95) = 9.25$, $p = .003$, $\eta_p^2 = 0.09$; however, in contrast with our hypothesis, RT was faster in go trials following SE trials than following go trials, mean difference$_{(pSE-pG)} = -18.18$ ms, 95%CI = [-30.04, −6.31]. In addition, there was a large-sized effect of Condition (pG, pSE) on accuracy, $F(1,95) = 39.39$, $p=<.001.$, $\eta_p^2 = 0.29$; again in contrast with our hypothesis, accuracy was lower in go trials following SE trials than following go trials, mean difference(pSE-pG) = −2.57%, 95%CI = [−3.38, −1.76]. These results indicate a speed-accuracy tradeoff, with post-error acceleration instead of slowing, while accuracy decreased. In a post-hoc analysis (see Supplementary Fig. 1), only in the first run participants slowed down after stop errors (but not after successful stops), while in the following five runs they increasingly speeded their responses after stop errors.

Number of artefact-free segments did not differ between groups for pG, pSE, and G response (respectively: mean = 216, 54, 365) and there were no differences in number of interpolations (mean = 1.5). For SE response, the TD group had more segments than the ADHD group (respectively: mean = 53, 48), $F(1,95) = 6.89$, $p=<.010$. Overall, the ERPs are reliable, as waveforms for odd and even trials are similar, see Supplementary Analyses.

3.2. ERP components

Mean amplitudes of the ERP components of the two groups are shown in Table 3 for each location and condition. Waveforms are shown in Fig. 2 (Ne, Pe) and Fig. 3 (N2). First, ERP components were validated for expected condition and location effects, without group distinction.

Ne (77–127 ms). Both timing and polarity are in line with the literature (Gehring et al., 2018; Overbye et al., 2019). Condition effects were dependent on scalp location, as described by Condition*Sagittal, $F(2,95) = 102.18$, $p < .001.$, $\eta_p^2 = 0.68$, and Condition*Lateral interactions, $F(2,95) = 23.87$, $p < .001.$, $\eta_p^2 = 0.33$. Post-hoc tests showed higher Ne amplitudes for SE trials than G trials in frontal, $F(1,96) = 126.31$, $p < .001.$, $\eta_p^2 = 0.57$, and central locations, $F(1,96) = 194.53$, $p < .001.$, $\eta_p^2 = 0.67$, but not in parietal locations, $F(1,96) = 2.24$, $p = 138.$, $\eta_p^2 = 0.02$. Condition effects were larger for midline locations than left, $F(1,96) = 36.17$, $p < .001.$, $\eta_p^2 = 0.27$, and right hemispheric locations, $F(1,96) = 23.28$, $p < .001.$, $\eta_p^2 = 0.20$, while left and right locations

Table 3
Mean amplitudes for Ne, Pe and N2 for TD and ADHD.

		TD			ADHD		
		G	SE	DIF	G	SE	DIF
Ne	F3	3.35 (2.83)	0.47 (3.25)	−2.89 (3.49)	2.43 (2.51)	−0.61 (2.73)	−3.04 (2.74)
	Fz	3.95 (3.32)	−0.67 (3.78)	−4.62 (3.75)	2.65 (2.79)	−1.15 (3.19)	−3.80 (3.08)
	F4	3.83 (2.85)	0.71 (3.01)	−3.12 (3.50)	2.73 (2.65)	−0.47 (2.81)	−3.20 (3.00)
	C3	0.79 (2.92)	−2.47 (2.84)	−3.26 (2.85)	0.79 (1.78)	−1.79 (2.37)	−2.58 (2.07)
	Cz	1.47 (3.06)	−2.95 (3.25)	−4.42 (3.29)	1.26 (2.47)	−2.24 (3.14)	−3.50 (2.56)
	C4	1.39 (3.26)	−1.92 (3.28)	−3.31 (3.07)	0.77 (1.85)	−2.24 (2.43)	−3.01 (2.53)
	P3	−4.91 (2.63)	−3.91 (2.52)	1.00 (3.09)	−3.46 (1.81)	−2.91 (2.43)	0.55 (2.38)
	Pz	−3.56 (2.54)	−3.73 (3.18)	−0.17 (2.80)	−3.25 (2.06)	−3.73 (2.65)	−0.47 (2.67)
	P4	−4.01 (2.32)	−3.09 (2.87)	0.92 (3.14)	−3.38 (2.04)	−3.22 (2.21)	0.16 (2.71)
Pe	F3	0.45 (4.25)	0.95 (5.46)	0.49 (7.37)	0.46 (3.68)	0.05 (3.89)	−0.41 (4.90)
	Fz	3.31 (5.03)	1.08 (5.28)	−2.23 (7.84)	1.91 (4.26)	0.19 (5.45)	−1.72 (5.88)
	F4	1.88 (3.75)	1.16 (4.69)	−0.71 (6.54)	1.04 (3.79)	0.11 (4.33)	−0.93 (5.20)
	C3	−4.89 (4.50)	0.02 (4.33)	4.92 (6.03)	−2.29 (3.37)	0.39 (3.36)	2.71 (5.15)
	Cz	−5.26 (4.72)	2.47 (4.13)	7.72 (5.99)	−2.94 (3.82)	0.90 (4.40)	3.86 (4.66)
	C4	−2.68 (4.26)	−0.04 (4.06)	2.66 (6.43)	−1.52 (3.08)	−0.90 (3.97)	0.63 (4.91)
	P3	−8.71 (5.21)	1.55 (3.85)	10.25 (6.34)	−6.29 (3.04)	1.73 (2.92)	8.02 (4.41)
	Pz	−8.28 (5.03)	3.15 (3.79)	11.42 (6.72)	−7.22 (3.04)	1.78 (4.33)	9.00 (5.02)
	P4	−6.73 (4.43)	1.21 (3.76)	7.94 (5.99)	−5.91 (2.71)	0.79 (4.03)	6.69 (5.25)
		pG	pSE	DIF	pG	pSE	DIF
N2	F3	−2.02 (5.92)	−4.52 (5.76)	−2.49 (5.47)	−3.60 (4.33)	−3.50 (6.02)	0.09 (5.49)
	Fz	−3.78 (5.55)	−5.85 (5.70)	−2.06 (5.55)	−4.25 (4.81)	−4.42 (7.15)	−0.16 (5.97)
	F4	−0.87 (5.46)	−2.60 (5.87)	−1.72 (5.28)	−2.46 (4.49)	−2.03 (6.38)	0.43 (5.34)
	C3	2.61 (6.20)	−0.05 (7.40)	−2.67 (5.19)	−0.83 (4.22)	−0.88 (5.71)	−0.05 (5.34)
	Cz	1.00 (6.33)	−2.03 (7.25)	−3.04 (5.51)	−1.62 (4.87)	−1.26 (6.65)	0.36 (5.04)
	C4	0.93 (6.10)	−1.78 (6.42)	−2.72 (4.48)	−1.27 (4.36)	−0.98 (5.46)	0.29 (4.91)
	P3	10.38 (6.53)	8.89 (7.96)	−1.48 (4.94)	6.54 (4.29)	7.11 (5.85)	0.57 (5.77)
	Pz	8.11 (6.51)	5.69 (7.49)	−2.42 (5.16)	5.23 (5.29)	6.52 (6.37)	1.28 (4.69)
	P4	9.27 (5.92)	6.62 (7.59)	−2.65 (4.80)	6.47 (4.92)	7.83 (5.28)	1.36 (4.60)

Note. Mean amplitudes in μV (*SD*) for response-locked Ne (77–127 ms) and Pe (420–520 ms), and stimulus-locked N2 (373–398 ms) for Frontal (F3, Fz, F4), Central (C3, Cz, C4), and Parietal (P3, Pz, P4) electrode locations. G = go; SE = stop error; DIF = difference (SE-G); pG = post go; pSE = post stop error; TD = typically developing.
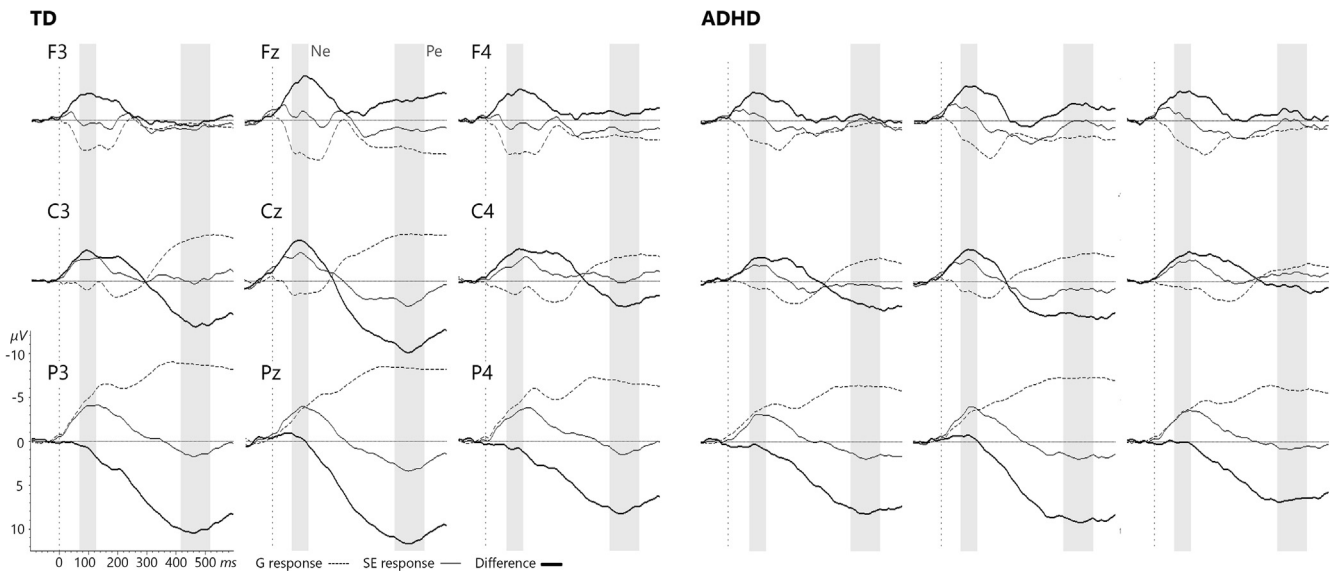

Fig. 2. Response-locked event-related potentials (ERPs) for correct go (G) and incorrect stop trials (SE) in the TD and ADHD group. *Note.* The image shows a grid of 9 electrodes that were used for statistical analyses, with Sagittal (top to bottom = anterior to posterior) and Lateral dimensions (left to right). The grey areas depict the time windows used for statistical analyses of Ne (77–127 ms) and Pe (420–520 ms). Effects of group were tested using the difference waves (SE-G) depicted in bold. TD = typically developing.

were similar, $F(1,96) = 0.88$, $p = .351.$, $\eta p^2 = 0.01$. Ne amplitude (SE-G) was larger for frontal versus parietal, $F(1,96) = 106.29$, $p < .001.$, $\eta p^2 = 0.53$, and midline versus parietal, $F(1,96) = 206.49$, $p < .001.$, $\eta p^2 = 0.68$, but not between frontal and central locations, $F(1,96) = 0.12$, $p = .73.$, $\eta p^2 = 0.00$. In summary, the Ne component demonstrated a frontocentral midline maximum for SE versus G trials.

Pe (420–520 ms). Both timing and polarity are in line with the literature (Ridderinkhof et al., 2009; Overbye et al., 2019). All main effects and interactions were significant, including the three-way interaction Condition*Sagittal*Lateral, $F(4,93) = 30.98$, $p < .001.$, $\eta p^2 = 0.57$. To interpret this three-way interaction, separate two-way interactions, Condition*Sagittal, were explored for different levels of Lateral (left, midline and right locations). These two-way interactions were significant for all levels of Lateral ($\eta p^2 = 0.64$, 0.59 and 0.60). Therefore, Condition effects were explored for all 9 electrodes. Pe amplitude was larger in SE trials than G trials for all central and parietal electrodes, while no statis-
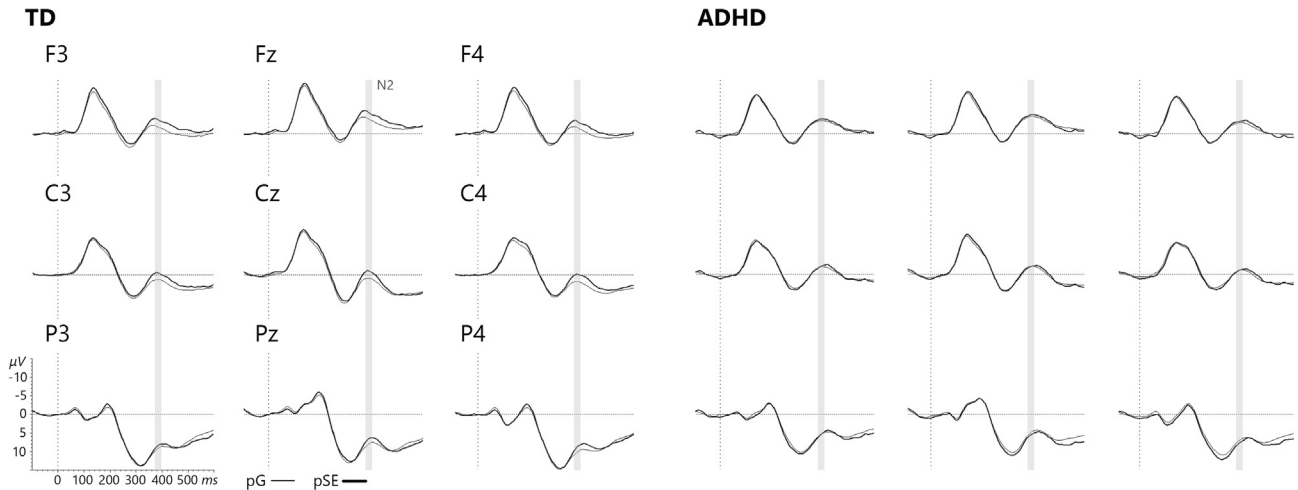
Fig. 3. Stimulus-locked event-related potentials (ERPs) for G trials following correct go trials (pG) and stop errors (pSE) in the TD and ADHD group. *Note.* The image shows a grid of 9 electrodes that were used for statistical analyses, with Sagittal (top to bottom = anterior to posterior) and Lateral dimensions (left to right). The grey area depicts the time window used for statistical analyses of N2. Visual inspection shows that only for the TD group, N2 amplitudes were larger for correct go trials when they were preceded by a stop error trial. TD = typically developing.

tical differences were demonstrated for left and right frontal electrodes (F3 and F4), and for Fz more positive amplitudes were found in G versus SE trials. To further test topographic effects of Pe, difference waves were calculated (SE-G) and Sagittal, $F(2,95) = 82.16$, $p < .001.$, $\eta p^2 = 0.63$, and Lateral effects, $F(2,95) = 14.88$, $p < .001.$, $\eta p^2 = 0.24$, were further explored. Pe amplitude was larger in parietal locations than middle, $F(1,96) = 136.43$, $p < .001.$, $\eta p^2 = 0.59$, and frontal locations, $F(1,96) = 150.60$, $p < .001.$, $\eta p^2 = 0.61$. Furthermore, Pe amplitude was larger for left, $F(1,96) = 9.40$, $p = .003.$, $\eta p^2 = 0.09$, and midline, $F(1,96) = 29.65$, $p < .001.$, $\eta p^2 = 0.24$, compared to right-hemispheric locations, while no differences were observed between left and midline locations, $F(1,96) = 0.81$, $p = .371$, $\eta p^2 = 0.01$. In summary, the Pe component demonstrated a parietal midline maximum, with s slight shift to the left hemisphere, for SE versus G trials.

N2 (373–398 ms). Polarity, topography and condition effects were in line with Chang et al. (2014), while the timing is more delayed. Condition effects were dependent on Sagittal locations, as described by the Condition*Sagittal interaction, $F(2,95) = 4.78$, $p = .011.$, $\eta p^2 = 0.09$. N2 amplitude was larger for pSE than pG in central locations, $F(1,96) = 7.98$, $p = .006.$, $\eta p^2 = 0.08$, near-significantly for frontal locations, $F(1,96) = 3.83$, $p = .053.$, $\eta p^2 = 0.04$, but not for parietal locations, $F(1,96) = 1.73$, $p = .192.$, $\eta p^2 = 0.02$. In addition, a main effect of Lateral was found, $F(2,95) = 19.23$, $p < .001.$, $\eta p^2 = 0.29$. Pairwise comparisons revealed more negative N2 amplitudes for midline locations than left and right-hemispheric locations, $p < .001$, while left and right locations were similar, $p = .706$. In summary, the N2 component demonstrated a frontal midline maximum, which was more pronounced for pSE than pG trials.
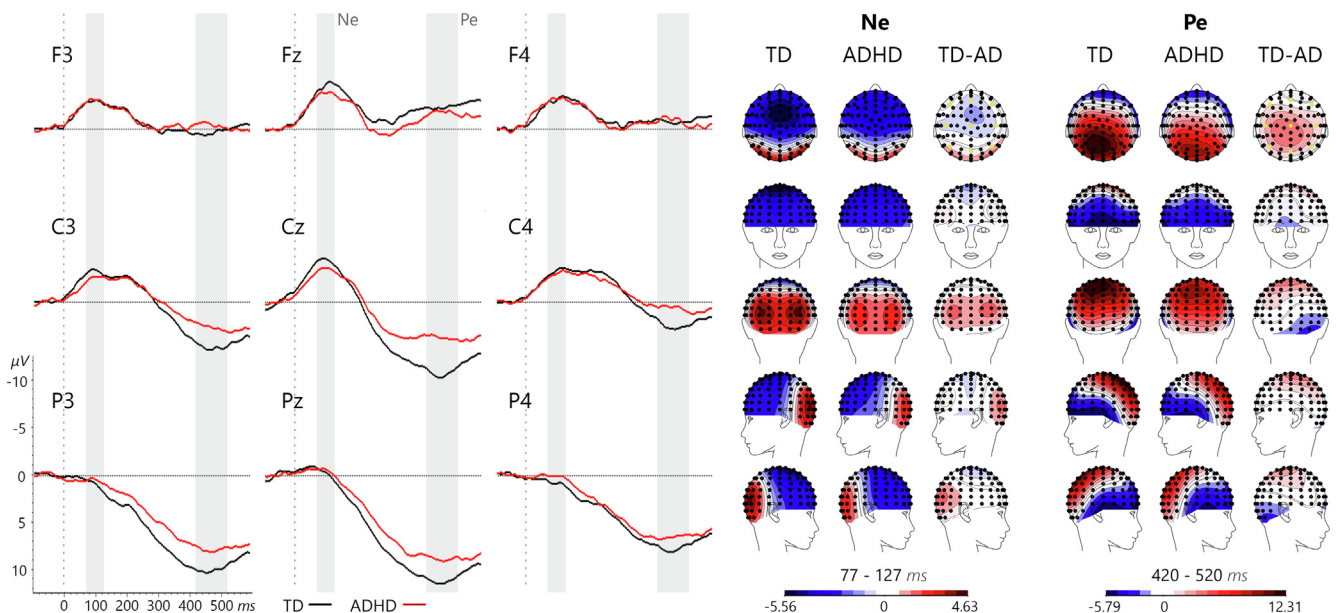

Fig. 4. Response-locked event-related potentials (ERPs) for the difference waves (SE-G) and topographic maps for the TD and ADHD group. *Note.* The image shows a grid of 9 electrodes that were used for statistical analyses, with Sagittal (top to bottom = anterior to posterior) and Lateral dimensions (left to right). The grey areas depict the time windows used for statistical analyses of Ne (77–127 ms) and Pe (420–520 ms). TD = typically developing.
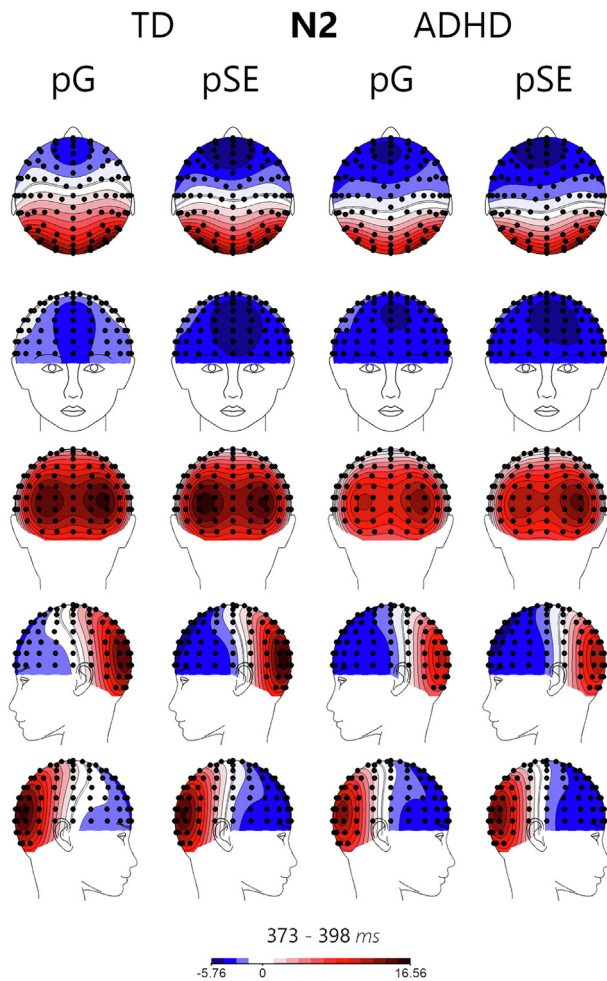
TD   **N2**   ADHD
pG   pSE   pG   pSE

373 - 398 *ms*

-5.76   0   16.56

Fig. 5. Topographic maps for the stimulus-locked N2 for the TD and ADHD group. *Note.* pG = correct go trial after another correct go trial; pSE = correct go trial after a stop error trial; TD = typically developing.

3.3. Group differences

Based on the first three MANOVAs, we concluded that Ne, Pe and N2 components are present in the data. For testing Group effects, midline electrodes (Fz, Cz, Pz) were used to reduce complexity (for argumentation, see Methods). Only Group effects, or interactions with Group are reported. See Figs. 4 and 5 for topographic maps of respectively Ne and Pe.

Ne (77–127 ms). No significant main effects of Group on Ne amplitude (SE-G), $F(1,95) = 1.06$, $p = .306$, $\eta p^2 = 0.01$, nor a significant interaction between Group*Location, $F(2,94) = 1.89$, $p = .157$, $\eta p^2 = 0.04$, were present.

Pe (420–520 ms). A large effect was found for the Group*Location interaction, $F(2,94) = 7.35$, $p = .001$, $\eta p^2 = 0.14$. Post-hoc tests showed similar Pe amplitudes for the ADHD and TD group for Fz, $F(1,95) = 0.13$, $p = .719$, $\eta p^2 = 0.00$; however, in line with our hypothesis, Pe amplitudes were reduced in the ADHD group for Cz, $F(1,95) = 12.42$, $p = .001$, $\eta p^2 = 0.12$, and Pz, $F(1,95) = 3.97$, $p = .049$, $\eta p^2 = 0.04$. The Pe reduction was large for the central electrode (Cz), mean difference$_{(TD-ADHD)}$ = 3.87 μV, 95%CI = [1.69, 6.05], and small/medium for the parietal electrode (Pz), mean difference$_{(TD-ADHD)}$ = 2.42 μV, 95%CI = [0.01, 4.83].

N2 (373–398 ms). A medium/large effect was found for the Group*Condition interaction, $F(1,95) = 10.14$, $p = .002$, $\eta p^2 = 0.10$. In line with our hypothesis, post-hoc tests demonstrated a large Condition effect only for the TD group, $F(1,50) = 15.51$, $p < .001$, $\eta p^2 = 0.24$, but not for the ADHD group, $F(1,45) = 0.50$, $p = .48$, $\eta p^2 = 0.01$. For the TD group, N2 amplitude was larger during pSE trials (correct go trials following stop errors) than pG trials (correct go trials following correct go trials), mean difference$_{(pSE-pG)}$ = 1.78 μV, 95%CI = [0.29, 3.27]. As can be seen in Fig. 3, although the N2 peak is more pronounced in the TD group (compared to the preceding positive wave), the N2 deflection in the ADHD group is shifted more to negative polarity. This is reflected in group differences for the pG Condition, $F(1,95) = 4.19$, $p = .04$, $\eta p^2 = 0.04$.

3.4. Relations between performance, behaviour and ERPs

Post-error RT increase/not increase. Both SE response-locked difference waves (SE-G: Ne, Pe) and stimulus-locked pSE (N2) components were explored as a function of whether reaction times increased (i) or did not increase (ni) in these go trials following SE trials (pSEi, pSEni). Although we lowered the threshold to a minimum of 15 EEG segments for each condition, 86% of children in the TD group and 63% of children in the ADHD group remained for the analysis. Age differed for the remaining participants, $F(1,71) = 6.12$, $p = .016$. Therefore, groups were matched on gender and age, resulting in two groups of $n = 28$ each. No main or interaction effects were found for Condition (i versus ni) and Group for Ne, Pe and N2.

Correlations between performance, ADHD symptoms and ERPs. See Table 4 for correlational outcomes, reported separately for the TD and ADHD group. Only $p < .01$ correlations are reported here. No significant correlations were found between ERP amplitudes/ADHD symptoms and performance outcomes, PES and PEA. For the TD group, teacher-rated inattention symptoms correlated with N2 amplitude difference (pSE-pG). Smaller negative differences and larger positive differences were related to better attention. Lastly, Ne amplitude difference was related to N2 amplitude difference in the ADHD group, and with N2 pSE amplitude in both groups. More negative Ne amplitude differences were related to more negative N2 amplitude (differences).

3.5. Source localization

Given the ERP findings of reduced Pe amplitudes in the ADHD group (Fig. 6A and B), this analysis window was used to explore the underlying sources in the brain. Fig. 6C shows the statistical parametric maps of the group comparisons. The ADHD group showed reduced activation in a dorsal region of the posterior cingulate (Brodmann area [BA] 31) extending anteriorly into BA24. Most of the significant nodes were located in BA31 (n = 12), while 5 were located in BA24. The maximum of the cluster was located in BA31 (Talairach coordinates: x = -11, y = -21, z = 43), $t(96) = 4.11$, $p < .0001$. No significant correlations were found between the average activity of the cluster and performance or symptom variables.

To further understand the N2 modulation only found in the TD group, N2 was localized in the TD group for pG and pSE conditions and statistical parametric maps were calculated for the comparison between the two conditions with paired sample t-tests for each node, see Supplementary Fig. 2. Significant ($p < .0004$) higher activations were found mainly in the left hemisphere, in the ventrolateral prefrontal cortex (VLPFC) and the angular gyrus, although most activations were mirrored in the right hemisphere to a lesser extent.

4. Discussion

Children with ADHD show inaccurate and inconsistent response styles across a wide variety of cognitive paradigms, which seem to

Table 4
Partial Pearson correlations (adjusted for age) between performance, behavioral and ERP variables for TD (grey) and ADHD (white).

		1	2	3	4	5	6	7	8	9	10
1	PES	___	.04	.05	.32*	.01	.13	.00	−.19	−.01	.01
2	PEA	−.06	___	.06	−.11	−.05	.02	−.04	−.04	−.07	−.05
3	SWAN-IN-P	−.07	−.00	___	.07	.31*	−.20	.12	−.09	−.02	.10
4	SWAN-IN-T	−.10	−.03	.42**	___	.04	.58**	−.07	−.04	−.03	−.19
5	SWAN-H/I-P	−.12	.03	.67***	.24	___	.23	.04	−.07	−.13	.16
6	SWAN-H/I-T	−.24	.03	.23	.80***	.23	___	−.34*	.06	−.19	−.32*
7	Ne_Fz_dif	−.16	−.03	.26	.17	.10	.25	___	−.05	.45**	.44**
8	Pe_Pz_dif	−.13	−.14	−.11	−.05	−.03	−.10	−.06	___	−.04	.00
9	N2_Fz_dif	−.01	.26	−.27	−.43**	−.23	−.20	.02	−.00	___	.75***
10	N2_Fz_SE	−.01	.27	−.09	−31*	−.10	.24	.37**	−.08	.55***	___

Note. Pearson correlations between performance, behavioral and ERP variables. ERP = event-related potential, PES = post-error slowing, PEA = post-error accuracy, SWAN = Strengths and Weaknesses of ADHD symptoms and Normal behavior scale, IN = inattention, H/I = hyperactivity/impulsivity, P = parents, T = teachers. Fz = frontal electrode, Pz = posterior electrode, dif = SE-G difference wave; TD = typically developing. Grey area: typically developing children, white area: ADHD children.
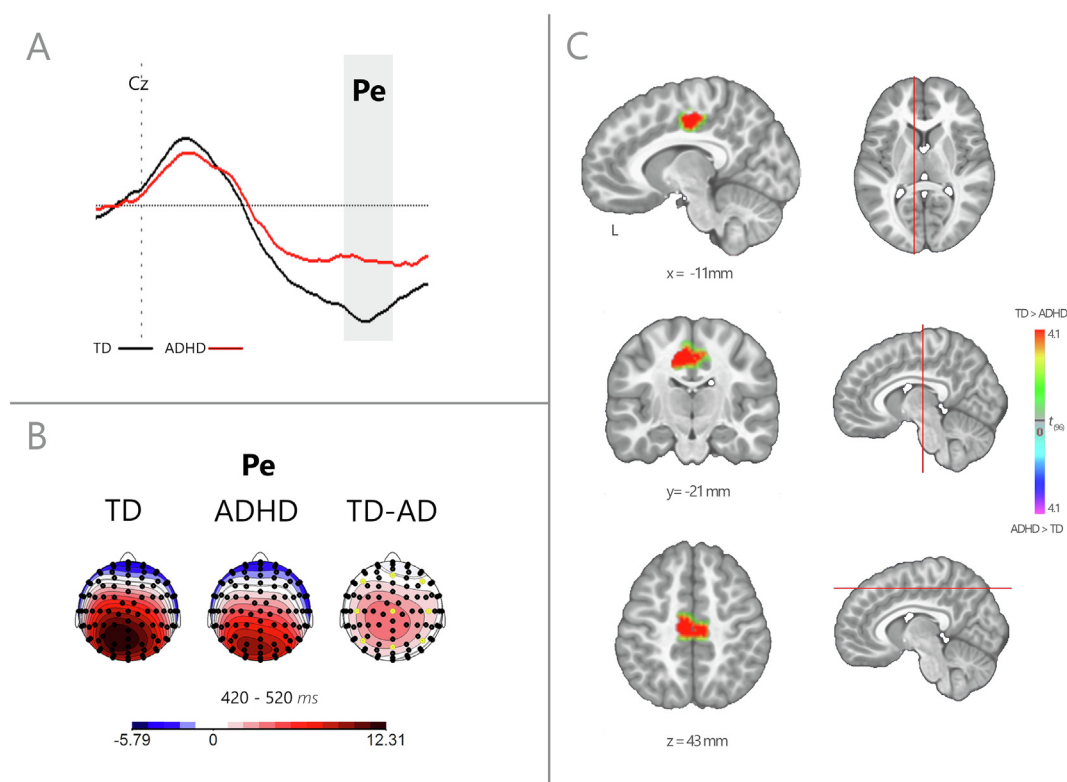* $p < .05$.
** $p < .01$.
*** $p < .001$.

Fig. 6. Statistical differences between ADHD and TD groups in source localization of Pe. *Note.* **A.** Vertex electrode (Cz) with the largest difference in Pe amplitude (difference wave: SE-GO) between the ADHD and TD group. The grey area is the time window used in further statistical tests; **B.** Top view of the topographic maps for the TD and ADHD group and group difference, based on the Pe time window. **C.** Significant differences between the ADHD and TD group in LAURA source estimations over the time window of Pe shown on a pediatric MNI template brain. Illustrated coordinates were converted from MNI to Talairach space. Color indicates t-values. Lower bound Bonferroni-corrected significance is $p < .0004$. For viewing purposes, images were interpolated with the 4NN method. TD = typically developing; MNI = Montreal Neurological Institute; 4NN = 4-nearest-neighbor.

transcend specific cognitive deficits found in each of these paradigms (Rommelse et al., 2007; Kofler et al., 2013). Regulatory deficit models of ADHD (Shiels and Hawk, 2010) try to explain these cross-paradigm findings. These models postulate that ADHD is characterized by deficits in *self-monitoring* and *adaptive control* processes that lead to impairments in goal-directed behavior. In the current study we used event-related potentials (ERP) indices of error processing (Ne: self-monitoring; Pe: adaptive control) and post-error processing (N2: implementation of cognitive control) to study these processes in children with ADHD. Overall, we

found evidence for a deficit in the later adaptive control process, as indicated by reduced Pe amplitudes in ADHD compared to TD children in response to errors. Group differences in Pe were localized in a region comprising the dorsal posterior (BA31) and midcingulate (BA24) cortex. In line with the adaptive control findings, children with ADHD did not modulate the N2 amplitude in trials following errors, while TD children did, indicating a deficit in implementation of cognitive control. We could not confirm the hypothesized differences in the earlier Ne component, nor did we find any behavioral evidence for deficits in adaptive control and

implementation of cognitive control, with similar behavioral adjustments in trials following errors (post-error slowing, PES; post-error accuracy; PEA) in both groups.

Although we expected to find a deficit in the earlier Ne component of error processing as well, the results of previously published studies are highly conflicting in this regard. Including the current study, half could not demonstrate reduced Ne amplitudes in ADHD (nine studies out of 18), while the other half did (see Table 1). This heterogeneity possibly indicates that methodological differences play a role. However, the age range of samples studied, the sample size of studies, and the type of tasks used are similar in studies showing and not showing reduced Ne amplitudes. In contrast to the developmental literature on ADHD, a meta-analysis in adults and adolescents with ADHD provided clear evidence for a reduction in both Ne and Pe amplitudes (Geburek et al., 2013). This may imply that deficits in error monitoring, reflected in the Ne, develop with increasing age. In line with this idea, in a recent cross-sectional study in healthy participants aged between 8 and 19 years, only the Ne amplitude increased with age, while the Pe remained constant (Overbye et al., 2019). Considering the protracted development of the Ne, children with ADHD may grow into deficit in adolescence and adulthood.

In line with our hypothesis and most of the literature (10 of 14 studies, see Table 1), children with ADHD showed reduced Pe amplitudes in response to errors, providing evidence for a deficit in the later adaptive control process. Based on distributed source localization of the Pe, children with ADHD demonstrated reduced activation in the dorsal part of the posterior cingulate (BA31) extending into the midcingulate (BA24). FMRI studies of failed inhibition and error processing in ADHD reported reduced activation in the posterior cingulate as well (Rubia et al., 2005, 2009, 2011), although it is not possible to directly link such findings to a specific process in time (such as the Pe), due to low temporal resolution of fMRI. Earlier work has identified the posterior cingulate cortex as a neural generator of the Pe in healthy controls (O'Connell et al., 2007; Vocat et al., 2008), being part of a more distributed network (Wessel, 2012). In line with the alleged adaptive control function of the Pe, the dorsal posterior cingulate is involved in detecting and responding to environmental events that may require a change in behavior and that are not part of the current cognitive set (Leech and Sharp, 2014). To our knowledge, the current study is the first to localize the neural generators of Pe differences in children with ADHD, while removing stimulus-related overlap to improve isolation of error-related processes.

Two ERP source localization studies in adults with ADHD found a Pe generator in the same posterior cingulate area (O'Connell et al., 2009) or more anterior in BA24 (Czobor et al., 2017). However, in those studies, differences between ADHD and controls were apparent in other areas: the ACC and right insula. Methodological differences complicate integrating our findings with those earlier adult studies. Importantly, stop stimulus-evoked activity may overlap with and confound the response-locked error components in the former studies, resulting in residual inhibition-related processing, as was noted by Czobor et al. (2017) as well. This is especially important in Go/Nogo and SST paradigms, considering that ADHD is associated with deficient response inhibition (Barkley, 1997). Moreover, there are indications that error processing starts with a rapid inhibitory control process that interrupts the current task-set representation (Wessel, 2018a). Thus, both response inhibition and error processing may depend partly on similar neural generators (Wessel, 2018b). Without removing this overlap, it is difficult to disentangle their contributions. For example, the right anterior insula, as reported by Czobor et al (2017), is often implicated in response inhibition deficits in ADHD (Hart et al., 2013).

While most studies exclusively focused on the neural correlates of error monitoring, relatively few investigated the neural underpinnings of how cognitive control is actually *implemented* in subsequent post-error trials (and how this relates to behavioural adjustments). Our results showed a large modulation of N2 only in the TD group, with increased N2 amplitudes in go trials following stop error trials. Similar N2 modulations have been found in healthy adults, although it is not yet clear whether it signifies increased cognitive control in response to more general conflict, independent of PES (Upton et al., 2010), or whether it is specific to errors and PES (Chang et al., 2014). Two fMRI studies investigated the neural correlates of PES and found the right ventrolateral prefrontal cortex (VLPFC) to play an important role (Li et al., 2008; Zhang et al., 2017). In the current study we localized the N2 sources and found the left VLPFC and angular gyrus to be more active during post-error trials in TD children. Although activations were bilateral, as in a previous fMRI study (Li et al., 2008), the asymmetry was in favour of the left hemisphere in our study, opposed to the right in the fMRI studies. The relationship between approach/avoidance motivation and asymmetric frontal cortical activity may explain this discrepancy (Kelley et al., 2017). We were surprised to find speeded reaction times in go trials following stop errors for both ADHD and TD children, accompanied by lower accuracy. This reflects a more risky response style, in line with approach motivation (left-lateralized), but contrasts to the post-error slowing observed in other studies, which is reflective of avoidance motivation (right-lateralized). Li et al. (2009) found a left-lateralized effect to be associated with speeded responses as well.

While the EEG findings in this study are consistent with a deficit in error processing in ADHD, more specifically in the later adaptive control function (reduced Pe, localized in the posterior cingulate), and a subsequent deficit in the *implementation* of cognitive control (no N2 modulation in post-error trials), interpretation of the behavioural indices is complicated. First, we could not demonstrate any differences in PES and PEA between ADHD and TD children. Although a recent meta-analysis found reduced PES in children and adults with ADHD (Balogh and Czobor, 2016), only 2 out of 8 ERP studies reported reduced PES in children with ADHD, while another 9 studies did not report post-error adjustment indices. One important factor that may explain the inconsistent findings is the different inter-stimulus-interval (ISI) used across studies as shown in the meta-analysis by Balogh and Czobor (2016). PES increases with longer intervals between stimuli in TD children, presumably because there is more time available to adjust behaviour after an error and therefore strategic influence can be more effective, while this effect is absent in ADHD (Balogh and Czobor, 2016). This means that effect-size differences between groups increase with longer ISI as well. Compared to the earlier studies, our ISI of 2400–2600 ms was relatively short and hence the expected effect size for PES differences was small. Although this may explain the absence of group differences, it cannot explain the unexpected speeding of reaction times and reduced accuracy across groups.

Two explanations are plausible for the speed-accuracy trade-off found in the current study. First, more recent theories on error processing propose that a general orienting response (OR) immediately follows errors, and dependent on task context and timing, this may have adaptive or maladaptive consequences (Ullsperger and Danielmeier, 2016; Wessel, 2018a). In his adaptive orienting theory of error processing, Wessel (2018a) proposes that all unexpected events, including errors, are followed by an automatic cascade that consists of two rapid, sequential processes - both of which are aimed at interrupting ongoing processing and shifting attention to the source of the unexpected event. The first process

is a rapid inhibitory control process, followed by attentional orienting. Although this automated cascade ultimately benefits controlled processing specific to errors, when the timing of the next stimulus is within this critical period, it can be decremental to performance. On a side note, deviant Ne/Pe findings in ADHD may actually represent inhibition and/or attention deficits when interpreted in light of this theory, rather than a specific deficit in error-monitoring (adaptive control). A second explanation is that in our version of the SST, stop trials never followed each other directly (a minimum of one go trial was placed in between stop trials). Children may have become aware of this and might have taken a more risky style of responding directly after each stop trial (knowing that no inhibition was needed). Our post-hoc analysis supports this explanation. While in the first run children slowed down after errors (mean 32 ms), in the following runs they speeded their reactions (−20 to −50 ms). This is in line with model-based fMRI suggesting that PES results from trial-by-trial updating of the probability of the stop signal (Ide et al., 2013). While awareness increased, children may have switched from avoidance to approach motivated behaviour. It is unknown whether other ERP studies of error processing in ADHD did or did not have stop trials directly following each other, as this is not explicitly reported, but it may be a source of heterogeneity.

Our particular version of the SST without completely random stop trials may be seen as a limitation, but also as an opportunity to learn new aspects about error processing and implementation of cognitive control in ADHD and TD children. First, we can conclude that error processing is affected in ADHD, even when controlled processing of the next stimulus is not required. Second, future studies could manipulate the occurrence and predictability of the stop signal to make or break the association between error processing and post-error slowing and accuracy in ADHD. By parametrically altering the predictability, it is possible to investigate a range of approach and avoidance-related strategies that are implemented after errors and conflict. Strengths of our study include a relatively large sample size, a well-defined ADHD sample with stringent inclusion criteria, removal of overlapping stop stimulus-evoked activity, individual distributed source localization and statistical comparisons between groups, and the additional analysis of how cognitive control is implemented in subsequent post-error trials.

In conclusion, we could not demonstrate early (Ne) processing differences of errors, while later (Pe) error processing, associated with adaptive control, was markedly reduced in children with ADHD and localized in the dorsal posterior cingulate. This was followed by a deficit in the *implementation* of cognitive control in post-error trials. While the TD group showed increased N2 amplitudes in go trials following stop error trials, localized in the left ventrolateral prefrontal cortex (VLPFC) and angular gyrus, the ADHD group did not. The behavioural indices of error processing, post-error slowing and accuracy, were not in line with the ERP results. Future studies could benefit from parametrically altering the predictability of the stop signal and the inter-stimulus-interval to test under what conditions errors result in (mal)adaptive behavioural adjustments in ADHD and TD children.

Acknowledgements

Declaration of Competing Interest

None.

Appendix A. Supplementary data

Supplementary data to this article can be found online at https://doi.org/10.1016/j.clinph.2020.06.022.

References

Albrecht B, Brandeis D, Uebel H, Heinrich H, Mueller UC, Hasselhorn M, et al. Action Monitoring in Boys With Attention-Deficit/Hyperactivity Disorder, Their Nonaffected Siblings, and Normal Control Subjects: Evidence for an Endophenotype. Biol Psychiatry 2008;64:615–25.

Althaus M, Groen Y, Wijers AA, Minderaa RB, Kema IP, Dijck JDA, et al. Variants of the SLC6A3 (DAT1) polymorphism affect performance monitoring-related cortical evoked potentials that are associated with ADHD. Biol Psychol 2010;85:19–32.

Arnett AB, Pennington BF, Friend A, Willcutt EG, Byrne B, Samuelsson S, et al. The SWAN Captures Variance at the Negative and Positive Ends of the ADHD Symptom Dimension. J Atten Disord 2013;17:152–62.

Balogh L, Czobor P. Post-Error Slowing in Patients With ADHD. J Atten Disord 2016;20:1004–16.

Barkley RA. Behavioral inhibition, sustained attention, and executive functions: Constructing a unifying theory of ADHD. Psychol Bull 1997;121:65–94.

Bekker EM, Kenemans JL, Hoeksma MR, Talsma D, Verbaten MN. The pure electrophysiology of stopping. Int J Psychophysiol 2005;55:191–8.

Birot G, Spinelli L, Vulliémoz S, Mégevand P, Brunet D, Seeck M, et al. Head model and electrical source imaging: A study of 38 epileptic patients. NeuroImage Clin 2014;5:77–83.

Botvinick MM, Braver TS, Barch DM, Carter CS, Cohen JD. Conflict monitoring and cognitive control. Psychol Rev 2001;108:624–52.

Braet W, Johnson KA, Tobin CT, Acheson R, McDonnell C, Hawi Z, et al. fMRI activation during response inhibition and error processing: the role of the DAT1 gene in typically developing adolescents and those diagnosed with ADHD. Neuropsychologia 2011;49:1641–50.

Burgio-Murphy A, Klorman R, Shaywitz SE, Fletcher JM, Marchione KE, Holahan J, et al. Error-related event-related potentials in children with attention-deficit hyperactivity disorder, oppositional defiant disorder, reading disorder, and math disorder. Biol Psychol 2007;75:75–86.

Bush G, Luu P, Posner MI. Cognitive and emotional influences in anterior cingulate cortex. Trends Cogn Sci 2000;4:215–22.

Chang A, Chen C-C, Li H-H, Li C-S-R. Event-Related Potentials for Post-Error and Post-Conflict Slowing. Rypma B, editor. PLoS One 2014;9:e99909.

Cohen J. Statistical power analysis for the behavioral sciences. 1988

Coles MGH, Scheffers MK, Holroyd CB. Why is there an ERN/Ne on correct trials? Response representations, stimulus-related components, and the theory of error-processing. Biol Psychol 2001;56:173–89.

Corp IBM. IBM SPSS Statistics for Windows. Armonk, NY: IBM Corp; 2015.

Cubillo A, Halari R, Ecker C, Giampietro V, Taylor E, Rubia K. Reduced activation and inter-regional functional connectivity of fronto-striatal networks in adults with childhood Attention-Deficit Hyperactivity Disorder (ADHD) and persisting symptoms during tasks of motor inhibition and cognitive switching. J Psychiatr Res 2010;44:629–39.

Czobor P, Kakuszi B, Németh K, Balogh L, Papp S, Tombor L, et al. Electrophysiological indices of aberrant error-processing in adults with ADHD: a new region of interest. Brain Imaging Behav 2017;11:1616–28.

Eichele H, Eichele T, Bjelland I, Høvik MF, Sørensen L, van Wageningen H, et al. Performance Monitoring in Medication-Naïve Children with Tourette Syndrome. Front Neurosci 2016;10:50.

Endrass T, Reuter B, Kathmann N. ERP correlates of conscious error recognition: Aware and unaware errors in an antisaccade task. Eur J Neurosci 2007;26:1714–20.

Falkenstein M, Hohnsbein J, Hoormann J, Blanke L. Effects of crossmodal divided attention on late ERP components. II. Error processing in choice reaction tasks. Electroencephalogr Clin Neurophysiol 1991;78:447–55.

Fonov V, Evans A, McKinstry R, Almli C, Collins D. Unbiased nonlinear average age-appropriate brain templates from birth to adulthood. Neuroimage 2009;47: S102.

Fonov V, Evans AC, Botteron K, Almli CR, McKinstry RC, Collins DL. Unbiased average age-appropriate atlases for pediatric studies. Neuroimage 2011;54:313–27.

Geburek AJ, Rist F, Gediga G, Stroux D, Pedersen A. Electrophysiological indices of error monitoring in juvenile and adult attention deficit hyperactivity disorder (ADHD)—A meta-analytic appraisal. Int J Psychophysiol 2013;87:349–62.

Gehring W, Goss B, Coles M. A neural system for error detection and compensation. Psychol Sci 1993;4:385–90.

Gehring WJ, Goss B, Coles MGH, Meyer DE, Donchin E. The Error-Related Negativity. Perspect Psychol Sci 2018;13:200–4.

Grave de Peralta Menendez R, Murray MM, Michel CM, Martuzzi R, Gonzalez Andino SL. Electrical neuroimaging based on biophysical constraints. Neuroimage. 2004;21:527–39.

Groen Y, Wijers AA, Mulder LJM, Waggeveld B, Minderaa RB, Althaus M. Error and feedback processing in children with ADHD and children with Autistic Spectrum Disorder: An EEG event-related potential study. Clin Neurophysiol 2008;119:2476–93.

Groom MJ, Liddle EB, Scerif G, Liddle PF, Batty MJ, Liotti M, et al. Motivational incentives and methylphenidate enhance electrophysiological correlates of error monitoring in children with attention deficit/hyperactivity disorder. J Child Psychol Psychiatry Allied Discip 2013;54:836–45.

Groom MJ, Scerif G, Liddle PF, Batty MJ, Liddle EB, Roberts KL, et al. Effects of Motivation and Medication on Electrophysiological Markers of Response Inhibition in Children with Attention-Deficit/Hyperactivity Disorder. Biol Psychiatry 2010;67:624–31.

Hansen PC. Analysis of Discrete Ill-Posed Problems by Means of the L-Curve. SIAM Review 1992;34:561–80.

Hart H, Radua J, Nakao T, Mataix-Cols D, Rubia K. Meta-analysis of functional magnetic resonance imaging studies of inhibition and attention in attention-deficit/hyperactivity disorder: exploring task-specific, stimulant medication, and age effects. JAMA Psychiatry 2013;70:185–98.

Herrmann MJ, Römmler J, Ehlis AC, Heidrich A, Fallgatter AJ. Source localization (LORETA) of the error-related-negativity (ERN/Ne) and positivity (Pe). Cogn Brain Res 2004;20:294–9.

Ide JS, Shenoy P, Yu AJ, Li C -s. R. Bayesian Prediction and Evaluation in the Anterior Cingulate Cortex. J Neurosci. 2013;33:2039–47.

Janssen T, Geladé K, van Mourik R, Maras A, Oosterlaan J. An ERP source imaging study of the oddball task in children with Attention Deficit/Hyperactivity Disorder. Clin Neurophysiol 2016;127:1351–7.

Janssen T, Heslenfeld D, van Mourik R, Geladé K, Maras A, Oosterlaan J. Alterations in the Ventral Attention Network During the Stop-Signal Task in Children With ADHD: An Event-Related Potential Source Imaging Study. J Atten Disord 2018;22:639–50.

Janssen T, Hillebrand A, Gouw A, Geladé K, Van Mourik R, Maras A, et al. Neural network topology in ADHD; evidence for maturational delay and default-mode network alterations. Clin Neurophysiol 2017;128:2258–67.

Jonkman LM, van Melis JJM, Kemner C, Markus CR. Methylphenidate improves deficient error evaluation in children with ADHD: An event-related brain potential study. Biol Psychol 2007;76:217–29.

Jung TP, Makeig S, Humphries C, Lee TW, McKeown MJ, Iragui V, et al. Removing electroencephalographic artifacts by blind source separation. Psychophysiology 2000;37:163–78.

Kelley NJ, Hortensius R, Schutter DJLG, Harmon-Jones E. The relationship of approach/avoidance motivation and asymmetric frontal cortical activity: A review of studies manipulating frontal asymmetry. Int J Psychophysiol 2017;119:19–30.

Kofler MJ, Rapport MD, Sarver DE, Raiker JS, Orban SA, Friedman LM, et al. Reaction time variability in ADHD: A meta-analytic review of 319 studies. Clin Psychol Rev 2013;33:795–811.

Laird AR, Fox PM, Price CJ, Glahn DC, Uecker AM, Lancaster JL, et al. ALE meta-analysis: controlling the false discovery rate and performing statistical contrasts. Hum Brain Mapp 2005;25:155–64.

Lancaster JL, Tordesillas-Gutiérrez D, Martinez M, Salinas F, Evans A, Zilles K, et al. Bias between MNI and Talairach coordinates analyzed using the ICBM-152 brain template. Hum Brain Mapp 2007;28:1194–205.

Leech R, Sharp DJ. The role of the posterior cingulate cortex in cognition and disease. Brain 2014;137:12–32.

Li CR, Huang C, Yan P, Paliwal P, Constable RT, Sinha R. Neural Correlates of Post-error Slowing during a Stop Signal Task: A Functional Magnetic Resonance Imaging Study. J Cogn Neurosci 2008;20:1021–9.

Li CSR, Chao HHA, Lee TW. Neural correlates of speeded as compared with delayed responses in a stop signal task: An indirect analog of risk taking and association with an anxiety trait. Cereb Cortex 2009;19:839–48.

Liao Y-C, Guo N-W, Chen S-J, Tsai H-F, Fang J-H, Chen J-J, et al. The Significance of Impulsive Error in Children With ADHD. Clin EEG Neurosci 2018;49:295–301.

Liotti M, Pliszka SR, Perez R, Kothmann D, Woldorff MG. Abnormal brain activity related to performance monitoring and error detection in children with ADHD. Cortex 2005;41:377–88.

Luck SJ. A closer look at averaging: convolution, latency variability, and overlap. In: An Introduction to the Event-Related Potential Technique. MIT press, 2014.

Nieuwenhuis S, Ridderinkhof KR, Blom J, Band GP, Kok A. Error-related brain potentials are differentially related to awareness of response errors: evidence from an antisaccade task. Psychophysiology 2001;38:752–60.

O'Connell RG, Bellgrove MA, Dockree PM, Lau A, Hester R, Garavan H, et al. The neural correlates of deficient error awareness in attention-deficit hyperactivity disorder (ADHD). Neuropsychologia 2009;47:1149–59.

O'Connell RG, Dockree PM, Bellgrove MA, Kelly SP, Hester R, Garavan H, et al. The role of cingulate cortex in the detection of errors with and without awareness: A high-density electrical mapping study. Eur J Neurosci 2007;25:2571–9.

Orr C, Hester R. Error-related anterior cingulate cortex activity and the prediction of conscious error awareness. Front Hum Neurosci 2012;6:1–12.

Overbeek TJM, Nieuwenhuis S, Ridderinkhof KR. Dissociable Components of Error Processing: On the functional significance of the Pe vis-à-vis the ERN/Ne. J Psychophysiol 2005;19:319–29.

Overbye K, Walhovd KB, Paus T, Fjell AM, Huster RJ, Tamnes CK. Error processing in the adolescent brain: Age-related differences in electrophysiology, behavioral adaptation, and brain morphology. Dev Cogn Neurosci 2019;38:100665.

Pelham WE, Gnagy EM, Greenslade K, Milich R. Teacher ratings of DSM-III-R symptoms for the disruptive behaviour disorder. J Am Acad Child Adolesc Psychiatry 1992;31:210–8.

Perrin F, Pernier J, Bertrand O, Echallier JF. Spherical splines for scalp potential and current density mapping. Electroencephalogr Clin Neurophysiol 1989;72:184–7.

Pliszka SR, Glahn DC, Semrud-Clikeman M, Franklin C, Perez R, Xiong J, et al. Neuroimaging of inhibitory control areas in children with attention deficit hyperactivity disorder who were treatment naive or in long-term treatment. Am J Psychiatry 2006;163:1052–60.

Rabbitt PM. Errors and error correction in choice-response tasks. J Exp Psychol 1966;71:264–72.

Ridderinkhof KR, Ramautar JR, Wijnen JG. To P(E) or not to P(E): a P3-like ERP component reflecting the processing of response errors. Psychophysiology 2009;46:531–8.

Rommelse NNJ, Altink ME, de Sonneville LMJ, Buschgens CJM, Buitelaar J, Oosterlaan J, et al. Are Motor Inhibition and Cognitive Flexibility Dead Ends in ADHD?. J Abnorm Child Psychol 2007;35:957–67.

Rosch KS, Hawk LW. The effects of performance-based rewards on neurophysiological correlates of stimulus, error, and feedback processing in children with ADHD. Psychophysiology 2013;50:1157–73.

Rubia K, Cubillo A, Smith A, Woolley J, Heyman I, Brammer M. Disorder-specific dysfunction in right inferior prefrontal cortex during two inhibition tasks in boys with attention-deficit hyperactivity disorder compared to boys with obsessive-compulsive disorder. Hum Brain Mapp 2010;31:287–99.

Rubia K, Halari R, Mohammad A, Taylor E, Brammer M. Methylphenidate normalizes frontocingulate underactivation during error processing in attention-deficit/hyperactivity disorder. Biol Psychiatry 2011;70:255–62.

Rubia K, Halari R, Smith AB, Mohammad M, Scott S, Brammer MJ. Shared and disorder-specific prefrontal abnormalities in boys with pure attention-deficit/hyperactivity disorder compared to boys with pure CD during interference inhibition and attention allocation. J Child Psychol Psychiatry 2009;50:669–78.

Rubia K, Smith A, Brammer M, Toone B, Taylor E. Abnormal brain activation during inhibition and error detection in medication-naive adolescents with ADHD. Am J Psychiatry 2005;162:1067–75.

Senderecka M, Grabowska A, Szewczyk J, Gerc K, Chmylak R. Response inhibition of children with ADHD in the stop-signal task: an event-related potential study. Int J Psychophysiol 2012;85:93–105.

Shaffer D, Fisher P, Lucas CP, Dulcan MK, Schwab-Stone ME. NIMH Diagnostic Interview Schedule for Children Version IV (NIMH DISC-IV): description, differences from previous versions, and reliability of some common diagnoses. J Am Acad Child Adolesc Psychiatry 2000;39:28–38.

Shen I-H, Tsai S-Y, Duann J-R. Inhibition control and error processing in children with attention deficit/hyperactivity disorder: an event-related potentials study. Int J Psychophysiol 2011;81:1–11.

Shephard E, Jackson GM, Groom MJ. The effects of co-occurring ADHD symptoms on electrophysiological correlates of cognitive control in young people with Tourette syndrome. J Neuropsychol 2016;10:223–38.

Shiels K, Hawk LW. Self-regulation in ADHD: The role of error processing. Clin Psychol Rev 2010;30:951–61.

Sokhadze EM, Baruth JM, Sears L, Sokhadze GE, El-Baz AS, Williams E, et al. Event-related potential study of attention regulation during illusory figure categorization task in ADHD, autism spectrum disorder, and typical children. J Neurother 2012;16:12–31.

Swanson JM, Schuck S, Mann M, Carlson C. Categorical and dimensional definitions and evaluations of symptoms of ADHD: The SNAP and SWAN Rating Scales. Univ California, Irvine. 2006; Available at: http://www.adhd.net.

Ullsperger M, Danielmeier C. Reducing Speed and Sight: How Adaptive Is Post-Error Slowing?. Neuron 2016;89:430–2.

Ullsperger M, Danielmeier C, Jocham G. Neurophysiology of performance monitoring and adaptive behavior. Physiol Rev 2014;94:35–79.

Upton DJ, Enticott PG, Croft RJ, Cooper NR, Fitzgerald PB. ERP correlates of response inhibition after-effects in the stop signal task. Exp Brain Res 2010;206:351–8.

van Meel CS, Heslenfeld DJ, Oosterlaan J, Sergeant JA. Adaptive control deficits in attention-deficit/hyperactivity disorder (ADHD): The role of error processing. Psychiatry Res 2007;151:211–20.

van Rooij D, Hartman CA, Mennes M, Oosterlaan J, Franke B, Rommelse N, et al. Altered neural connectivity during response inhibition in adolescents with attention-deficit/hyperactivity disorder and their unaffected siblings. NeuroImage Clin 2015a;7:325–35.

van Rooij D, Hoekstra PJ, Mennes M, von Rhein D, Thissen AJAM, Heslenfeld D, et al. Distinguishing Adolescents With ADHD From Their Unaffected Siblings and Healthy Comparison Subjects by Neural Activation Patterns During Response Inhibition. Am J Psychiatry 2015b;172:674–83.

Van Veen V, Carter CS. The Timing of Action-Monitoring Processes in the Anterior Cingulate Cortex. J Cogn Neurosci 2002;14:593–602.

Vasey Michael W, Thayer Julian F. The Continuing Problem of False Positives in Repeated Measures ANOVA in Psychophysiology: A Multivariate Solution.

Psychophysiology 1987;24:479–86. https://doi.org/10.1111/j.1469-8986.1987.tb00324.x.

Verbruggen F, Chambers CD, Logan GD. Fictitious inhibitory differences: how skewness and slowing distort the estimation of stopping latencies. Psychol Sci 2013;24:352–62.

Vocat R, Pourtois G, Vuilleumier P. Unavoidable errors: A spatio-temporal analysis of time-course and neural sources of evoked potentials associated with error processing in a speeded task. Neuropsychologia 2008;46:2545–55.

Van De Voorde S, Roeyers H, Wiersema JR. Error monitoring in children with ADHD or reading disorder: An event-related potential study. Biol Psychol 2010;84:176–85.

Wechsler D. Weschler intelligence scale for children -. third edition. San Antonio, TXC: Psychological Corporation; 1991.

Wessel JR. Error awareness and the error-related negativity: evaluating the first decade of evidence. Front Hum Neurosci 2012;6:1–16.

Wessel JR. An adaptive orienting theory of error processing. Psychophysiology 2018a;55:1–21.

Wessel JR. Testing Multiple Psychological Processes for Common Neural Mechanisms Using EEG and Independent Component Analysis. Brain Topogr 2018b;31:90–100.

Wiersema JR, Van Der Meere JJ, Roeyers H. ERP correlates of impaired error monitoring in children with ADHD. J Neural Transm 2005;112:1417–30.

Woldorff MG. Distortion of ERP averages due to overlap from temporally adjacent ERPs: Analysis and correction. Psychophysiology 1993;30:98–119.

Yeung N, Botvinick MM, Cohen JD. The Neural Basis of Error Detection: Conflict Monitoring and the Error-Related Negativity. Psychol Rev 2004;111:931–59.

Zhang JS, Wang Y, Cai RG, Yan CH. The brain regulation mechanism of error monitoring in impulsive children with ADHD-An analysis of error related potentials. Neurosci Lett 2009;460:11–5.

Zhang Y, Ide JS, Zhang S, Hu S, Valchev NS, Tang X, et al. Distinct neural processes support post-success and post-error slowing in the stop signal task. Neuroscience 2017;357:273–84.